www.elsevier.com/locate/jobe

Effect of Climate and Design parameters on the Temperature Distribution of a Room

Fayadh Mohammed Abed, Omer Khalil Ahmed, Ahmed Emad Ahmed

PII: S2352-7102(17)30309-1
DOI: https://doi.org/10.1016/j.jobe.2018.02.007
Reference: JOBE410

To appear in: *Journal of Building Engineering*

Received date: 31 May 2017
Revised date: 6 February 2018
Accepted date: 10 February 2018

Cite this article as: Fayadh Mohammed Abed, Omer Khalil Ahmed and Ahmed Emad Ahmed, Effect of Climate and Design parameters on the Temperature Distribution of a Room, *Journal of Building Engineering,* https://doi.org/10.1016/j.jobe.2018.02.007

Effect of Climate and Design parameters on the Temperature Distribution of a Room

Dr. Fayadh Mohammed Abed[a], Dr. Omer Khalil Ahmed[b], Ahmed Emad Ahmed[c]

[a]Professor, University of Tikrit, Iraq-Salahdeen-Tikrit

[b]Assist Professor, Northern Technical university, Iraq-Kirkuk-Hawija

[c]Master student, University of Tikrit, Iraq-Salahdeen-Tikrit

Abstract

In the hot climate countries, like Iraq where solar energy is available at large levels, solar radiation represents the most important factor of cooling load in the building. The purpose of this paper is to determine the effect of size and orientation of the window on the temperature distribution and air velocity of rooms in Kirkuk city (35.47 ^{o}N, 44.39 ^{o}E), in north Iraq. The experimental investigation contained manufacturing four test rooms where the volume of each room was 1 m^3 and the window areas were 25%, 50%, 75%, and 100% from facade area. The test rooms were directed in west and south directions. A numerical analysis was carried out using the Fluent software and these results were validated by comparing it with the experimental results. The hourly system performance parameters were investigated for all test situations. The results of the study showed that the window size and its direction had a great effect on the temperature distribution of the experimental rooms; also, the results showed positive effect by directing the window to the south compared with the west direction. Both results of experimental and simulation showed that the average air temperature inside test room increased during time until 2 p.m. and then decreased. Besides, the results showed that the room with 25% of the facade had the best performance in comparison with other designs. A comparison indicates a good agreement of both experimental and simulation results.

Keywords: Climate, Design, Parameters, Window sizes, Temperature distribution.

Nomenclature

Symbol	Description Units
C_p	Specific heat J/kg.K
g	Acceleration due to gravity m/s^2
K	Thermal conductivity W/m.K
L_i	Thickness of insulation m
M	Mass kg
M_{tot}	Mass of air in test room kg
P	Pressure Pa
Ra	Rayleigh number (Gr.Pr) -

S	Source term -
t	Time s
T	Temperature ^{o}C
u	Velocity component in x-direction m/s
U	Property -
v	Velocity component in y-direction m/s
w	Velocity component in z-direction m/s
w_R	Uncertainty %
β	Coefficient of thermal expansion K^{-1}
Γ	Diffusion coefficient -
μ	Dynamic viscosity kg/m.s
ν	Kinematic viscosity m^2/s
ϕ	General Variable -
ρ	Density kg/m^3

Subscripts & Superscripts

Symbol	**Description**
av	Initial
o	Reference value
tot	Total

1. Introduction

In the hot climate regions like Iraq, where solar energy is available at large levels, solar radiation represents the most important factor of cooling load in a building[1]. The value of solar radiation entering the building through windows defines the energy consumptions for air conditioning in the building [2]. In the northern hemisphere, the windows are generally facing the south to receive ultimate sunlight during the cold season. Windows have a double function, permitting the solar radiation to increase the heating loads during winter season, and adding to house loads during summer season. Windows also perform a principle reason of heat loss in cold days [3].

The effect of window size on the thermal performance of the room is an interesting challenge facing researchers, where several studies have been conducted for this purpose[4]. Inanici, M.N. and Demirbilek, F.N. [2] presented an article to find the ideal construction aspect ratios and the effect of window sizes at south orientation on thermal performance of the building. Six various house aspect ratios and eight various south window sizes for each house were studied using SUNCODE-PC program in five Turkish cities. The data obtained were estimated in terms of total energy consumption while the ideal values were driven. Vedavyasa, M. et al. [5] studied the action of outlet window position on the temperature inside a room. It was noticed that the ratio of height of the window to the

height of wall (h/H = 0.33) gave a lower temperature index when the surface absorptivity decreased at the external walls.

Amos-Abanyie, S. et al. [6] viewed the effects of thermal mass, window size, and night ventilation at the peak of indoor air temperature in a humid warm climate in Ghana. Many of the experiments in the cooling load were conducted because most of these buildings were built using sand block. The simulation program (Energy Plus simulation software (E+)) was used to investigate the action of performance parameters (ventilation, window size and thermal mass) at night for temperature distribution.

Mari-Louise Persson et al. [7] used a dynamic building simulation tool (DEROB-LTH) to simulate a low energy demand for the building. The results showed that the area of the windows did not have the main operator on the warming requirement in the cold season but is pertinent for the cooling necessity in the hot season. To minimize the hazard of supernumerary temperature or energy requirement for cooling, there is an ideal window size directed to the south, lower than the main size of the inspected rooms. R.M.J. Bokel [8] presented an article to evaluate the yearly energy requirements for air conditioning and electric lighting as a function of window location, area, and the of the building in Netherlands. The data obtained can be used as the design of enhancement independent frontispiece for houses.

Farraj F. Al-ajmi and V.I. Hanby [9] utilized the TRNSYS-IISIBAT environment to achieve a building model in Kuwait city. A typical Kuwaiti meteorological data was intended and utilized to portend the cooling loads of an air-conditioned house. Numerical results have shown the eligible lineaments that should be adopted in domestic houses, with a view to alliterate the energy consumption code. Goopyo Hong et al. [10] analyzed the thermal performance of window systems using advanced system measurements. The results from the model utilized in the article proved that the thermal performance of window designs can be enhanced by utilizing perfect insulated or thermally broken barriers.

Salem bin Abdul Aziz al-Sudais[11] studied the effect of the orientation and area of the window on the thermal performance of the internal gaps in the houses built in hot areas. Five rooms were built for this purpose. The window area show that when the glass window forms 25% of the area of the southern façade, it is better to use a one-layer glass, two-layer glass is better for a 50% space window, and three-layers glass is better for 75% or 100% window area. Nazar Farag Antwan [12] presented a paper on the action of window over-hang in Iraqi house on cooling load. This study stated that limited width of over hang on south window diminishes the cooling load by 9%, and increases the width of the overhang to the east or west window to reduce the cooling load by the same percentage.

Koranteng, C. et al [13] explained a fulfillment into the importance of window sizes and its positioning on indoor temperature distribution for domestic buildings in Ghana. An exemplary cell of 3 m * 4 m was analyzed using the T_{as} tool. Different window sizes with different window areas to wall area ratios (WWR) were then inserted into different locations. The result showed that the optimum

window to wall ratio for realizing nearly comfortable indoor conditions should be between 10 to 40%. Shaik, S. [14] studied the thermal performance of different single glazing window glasses covered with and without window overhang shading. Five glass types were tested and the Energy plus 8.1 programs were used for this task. The results assisted in choosing the preferable window glass material as well as suitable dimensions for overhang shading system to reduce cooling loads in housing.

The purpose of this paper is to determine the effect of window size and its orientation on temperature distribution and air movement inside the rooms using both simulation and experimental approaches under Iraqi climate conditions to minimize cooling load from an energy perspective. This paper aims to provide architects with rules of thumbs of window design responding to the hot climate. It also contributes to the improvement of the conditions of the internal environment of the human.

2. Methodology

The goal of this article is to investigate experimentally and numerically the effect of window area and its direction on the temperature and velocity distributions inside rooms under the Iraqi hot climate. The summary of this study is as follows: in Section 2, the weather of study region, the experimental work, and the plane of tests are described, in Section 3, the mathematical model and Fluent program are presented. The results are shown and explained in Section 4 and the conclusion is summarized in Section 5.

2.1 Climate characteristics of the region

The experimental tests were conducted in Kirkuk city (35 ^{o}N, 44 ^{o}E); in the north of Iraq where the Summers are sultry, arid, and semi-dusty and the Winters are relatively cold and partly cloudy. Temperature ranges during the year are between 5 °C to 43 °C and sometimes below 1°C or above 46°C as shown in Fig.1 [15]. The hot season continues for 3.5 months, from 1 June to 15 September, with a mean daily high temperature above 37 °C. The cool season continues for four months, from 15-November to 15-March, with a mean high temperature lower than 19 °C. The chilly day of the year is on 23 January, with a mean lower than 5°C and higher than 13 °C [16]. The wind velocity at any region depends highly on earth topography, pressure-gradient force, and Coriolis force [17].

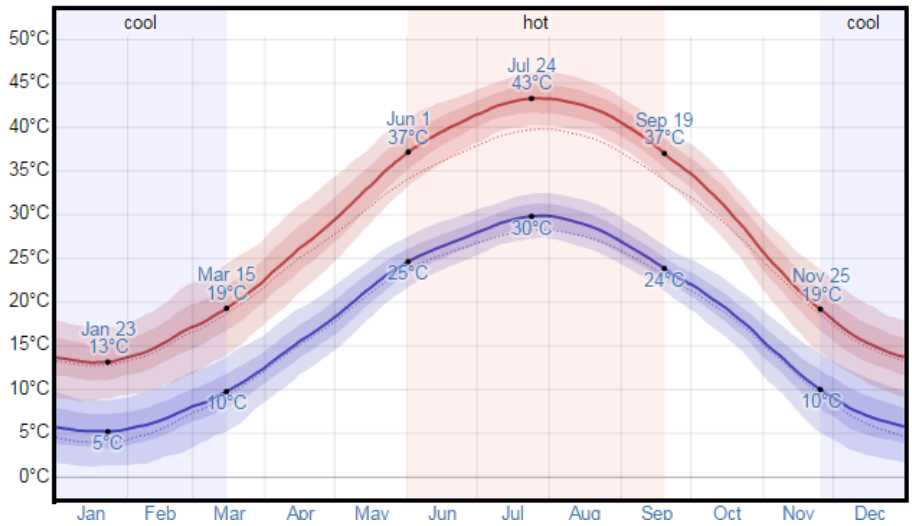

Fig. 1 Variation of the daily average maximum (red color) and low (blue color) temperature for study region[15]

Winds in the region of study are characterized by northwesterly and southwesterly winds coming from the Mediterranean Sea and southeast dusty winds have a significant impact on the climate throughout the year. The wind trends at in the study region are shown in Fig.2. The yearly average wind speeds are more than 6.9 kilometers per hour [18]. The windiest day of the year is on 27 June, with a mean hourly wind velocity of 7.9 kilometers per hour. In December, it is about 5 km/h [18]. The climate in the region of study is characterized by the presence of semi-vertical solar radiation, which ranges from 800 W/m^2 to 900 W/m^2 during the summer season. The sun brightness is up to 12 hours a day during July [19].

2-2 Description of experimental set-up:

For the purpose of the study of the distribution and thermal performance in the rooms, the test rooms were manufactured according to the standard specifications approved in the home industry [20]. Four test rooms were constructed with thermally insulated walls of 1 m^2 and 5 cm thickness for each face as shown in Fig. 3. The interior and exterior of the panels were made of zinc-coated aluminum and contained foam material. The rooms differed from each other according to the size of the windows. The size of the window varied from 25, 50, 70, and 100% of the wall area. The materials of these panels were lightweight, easy to apply and had high hardness and less thermal conductivity than others. Its thermal conductivity did not exceed 0.032 W/m.^{o}C and was calculated by thermal conductivity meters type (Fox 200).

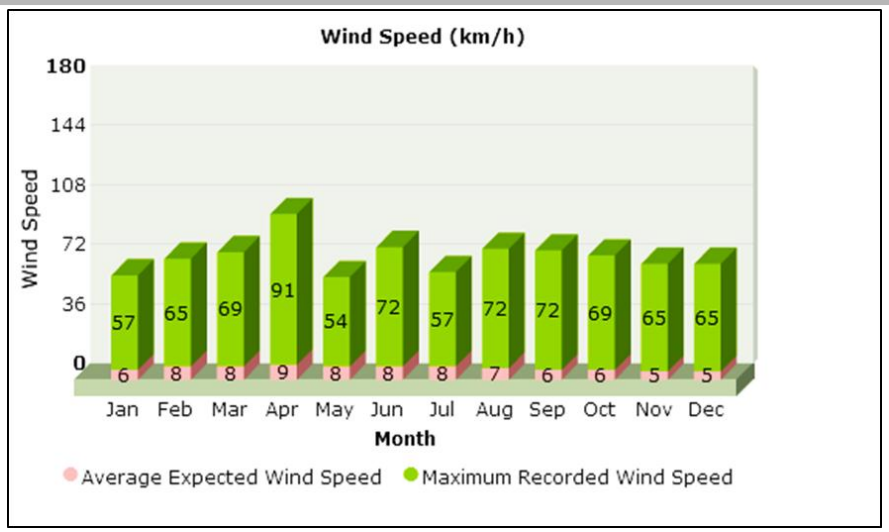

Fig. 20: Monthly wind speed average for the study region [18].

(A) Test rooms

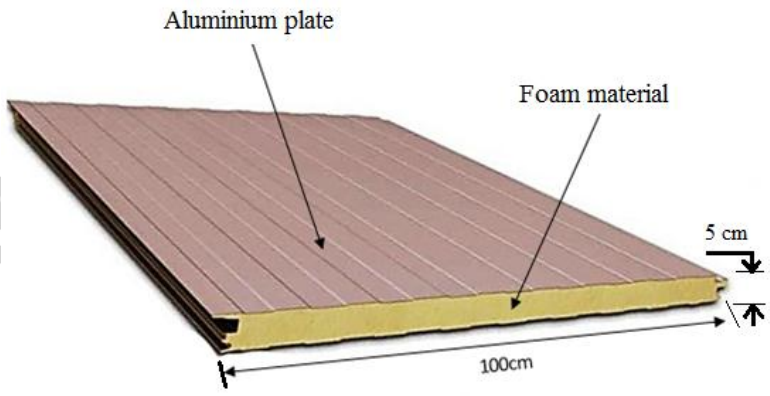

(B) Material of sandwich panel

Fig. 3: Photographic pictures of experimental setup

Eight thermocouple types (k) were utilized to sense the temperature in each experimental room. Two of the sensors were fixed in the mid-plane of each experimental room; the distance between them was 32 cm. The first sensor was fixed at 32 cm from the lower surface and the second sensor was fixed at 32 cm from the first sensor. This thermocouple, which was used in the experimental work,

calibrated against a standard mercury thermometer. These readings were represented in the calibration curve shown in Fig. 4. In order to record thermocouple readings, the thermocouple data logger (TC-08) was used for this purpose. The device contains eight channels through which eight reading units can be inserted and measured at the same time. Calculating the uncertainty in the experiment is very important for the validity of the analysis. Table 1 represents the uncertainty of the tools which are used in the experiments. The uncertainty of the obtained results is calculated by the following equation [21]:

$$\omega_R = \sqrt{\left(\frac{\partial U}{\partial x_1} \times w_1\right)^2 + \left(\frac{\partial U}{\partial x_2} \times w_2\right)^2 + \ldots\ldots\left(\frac{\partial U}{\partial x_n} \times w_n\right)^2} \quad (1)$$

Table (1) Uncertainty of the experimental apparatus

Equipment	Measurement	Error
Solar meter (SM206)	Solar radiation	(±3%)
Data logger	Voltage	(± 0.2%)
Thermocouples	Temperature	(±0.5 °C)

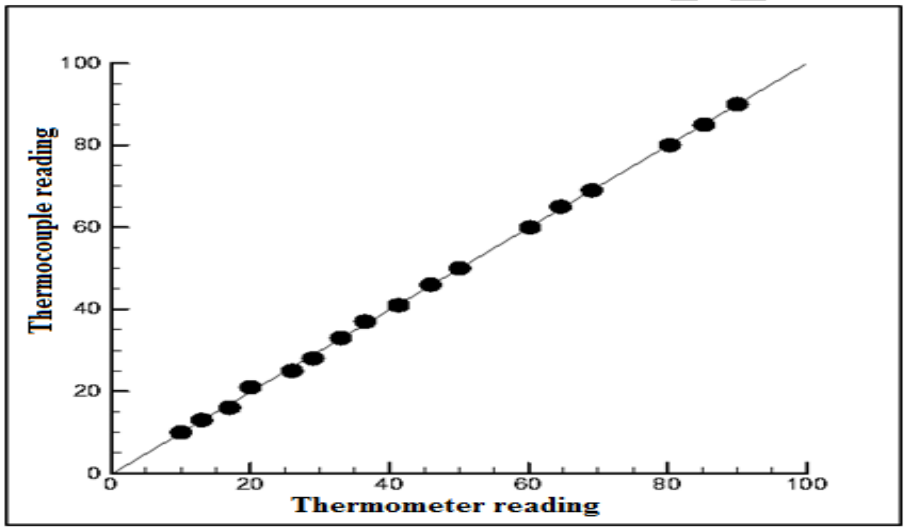

Fig. 4: Calibration curve of the thermocouples

2.3 Plane of Tests

The tests were carried out on selected clear sunny days in May, June, and July 2015. The experiment rooms were checked under steady-state status in which the weather conditions like solar intensity, wind speed, and the ambient temperature were treated as a constant for a period of time. At the beginning of each test, the glass cover of the test rooms was cleaned thoroughly and temperature measurements were checked and the test rooms faced south. Each experiment starts at sunrise and ends at sunset on the day of experimentation. The experimental parameters registered at the end of each hour included the solar radiation, ambient temperature, and the inside temperature of the test rooms.

3. Mathematical Model

Heat transfer in an enclosed space is complicated by the fact that the flow characteristics of a confined fluid are usually three-dimensional. Three-dimensional analysis is a difficult task because the non-linear momentum equations must be solved in addition to the mass and energy equations. The boundary conditions are also much more complicated than two-dimensional convection. As fluid is heated, there is an associated variation in the air density. The buoyancy effect due to this density change produces natural current resulting in the fluid motion relative to the bounding solid walls [22]. The buoyancy forces behave as body forces are included as such in the momentum equation. Under such conditions, the energy equation, continuity and momentum equations are coupled.

The fluid motion is presumed to be turbulent because of the large volume of the test rooms, three dimensional, and no internal heat generations while for appropriateness, the effects of radiation and viscous energy dissipation were ignored. With these hypotheses, the requisite convection equations are[23]:

1- Continuity Equation:

$$\frac{\partial u}{\partial t}+\frac{\partial u}{\partial x}+\frac{\partial v}{\partial y}+\frac{\partial w}{\partial z}=0 \tag{2}$$

2- Momentum equations:

$$\frac{\partial u}{\partial t}+u\frac{\partial u}{\partial x}+v\frac{\partial u}{\partial y}+w\frac{\partial u}{\partial z}=-\frac{1}{\rho}\frac{\partial p}{\partial x}+\nu\left[\frac{\partial^2 u}{\partial x^2}+\frac{\partial^2 u}{\partial y^2}+\frac{\partial^2 u}{\partial z^2}\right]$$

$$\frac{\partial v}{\partial t}+u\frac{\partial v}{\partial x}+v\frac{\partial v}{\partial y}+w\frac{\partial v}{\partial z}=-\frac{1}{\rho}\frac{\partial p}{\partial y}+g\beta(T-T_o)+\nu\left[\frac{\partial^2 v}{\partial x^2}+\frac{\partial^2 v}{\partial y^2}+\frac{\partial^2 v}{\partial z^2}\right] \tag{3}$$

$$\frac{\partial w}{\partial t}+u\frac{\partial w}{\partial x}+v\frac{\partial w}{\partial y}+w\frac{\partial w}{\partial z}=-\frac{1}{\rho}\frac{\partial p}{\partial z}+\nu\left[\frac{\partial^2 w}{\partial x^2}+\frac{\partial^2 w}{\partial y^2}+\frac{\partial^2 w}{\partial z^2}\right]$$

3- Energy equation:

$$\frac{\partial T}{\partial t}+u\frac{\partial T}{\partial x}+v\frac{\partial T}{\partial y}+w\frac{\partial T}{\partial z}=\frac{K}{\rho * C_p}\left[\frac{\partial^2 T}{\partial x^2}+\frac{\partial^2 T}{\partial y^2}+\frac{\partial^2 T}{\partial z^2}\right] \tag{4}$$

In the finite volume method, the above equations are treated in a balanced form for finite-sized control volumes (CV). Equations 1, 2, and 3 can be re-written as[23]:

$$\frac{\partial(\rho\phi)}{\partial t}+\frac{\partial(\rho u\phi)}{\partial x}+\frac{\partial(\rho v\phi)}{\partial y}+\frac{\partial(\rho w\phi)}{\partial z}=\frac{\partial}{\partial x}(\Gamma\frac{\partial\phi}{\partial x})+\frac{\partial}{\partial y}(\Gamma\frac{\partial\phi}{\partial y})+\frac{\partial}{\partial z}(\Gamma\frac{\partial\phi}{\partial z})+S \tag{5}$$

The fully implicit discretization equation for a typical control volume is shown as follows:

$$a_P\phi_P=a_W\phi_W+a_E\phi_E+a_S\phi_S+a_N\phi_N+a_B\phi_B+a_T\phi_T+a_P^0\phi_P^0+S_u \tag{6}$$

The coefficients of eq. (6) are given as follows:

a_w	$\text{Max}[F_w , (D_w+F_w/2) , 0]$
a_E	$\text{Max}[-F_e , (D_e- F_e/2) , 0]$
a_S	$\text{Max}[F_s , (D_s+F_s/2) , 0]$
a_N	$\text{Max}[-F_n , (D_n-F_n/2) , 0]$
a_B	$\text{Max}[F_b , (D_b+F_b/2) , 0]$
a_T	$\text{Max}[-F_t , (D_t-F_t/2) , 0]$
ΔF	$F_e - F_w + F_n - F_s + F_t - F_b$

The volume and cell face areas given in Fig. (5). the value of (F) and (D) are calculated from the following formula:

Face	w	e	s	n	b	t
F	$(\rho u)_w A_w$	$(\rho u)_e A_e$	$(\rho v)_s A_s$	$(\rho v)_n A_n$	$(\rho w)_b A_b$	$(\rho w)_t A_t$
D	$\frac{\Gamma_w}{\delta_{x_{WP}}} A_w$	$\frac{\Gamma_e}{\delta_{x_{PE}}} A_e$	$\frac{\Gamma_s}{\delta_{y_{SP}}} A_s$	$\frac{\Gamma_n}{\delta_{x_{PN}}} A_n$	$\frac{\Gamma_b}{\delta_{z_{BP}}} A_b$	$\frac{\Gamma_t}{\delta_{z_{PT}}} A_t$

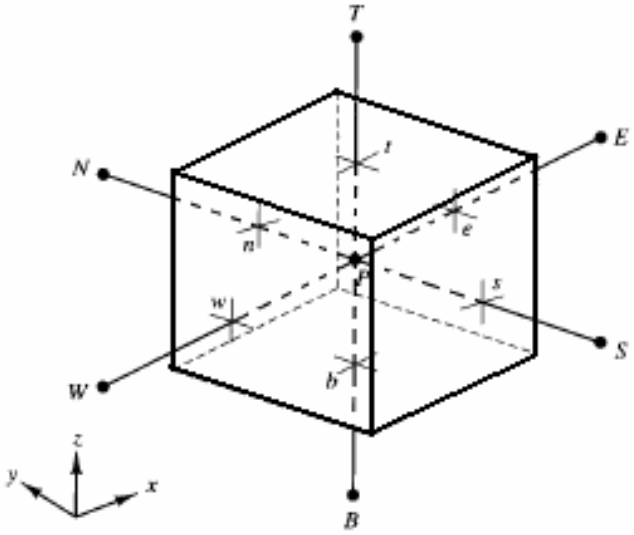

Fig.(5) Control volume used to illustrate discretization of a scalar transport equation

To select the discretization algorithm for the convection expression of each governing equation, the FLUENT package contains many discretization schemes. The three-dimensional shape of the experimental room needs computational fluid dynamic (CFD) program, Fluent, and the associated program for mesh building, Gambit. Gambit was used for generating the grid of the test rooms as shown in Fig.6. The grid density is much higher around the south face of the experimental rooms.

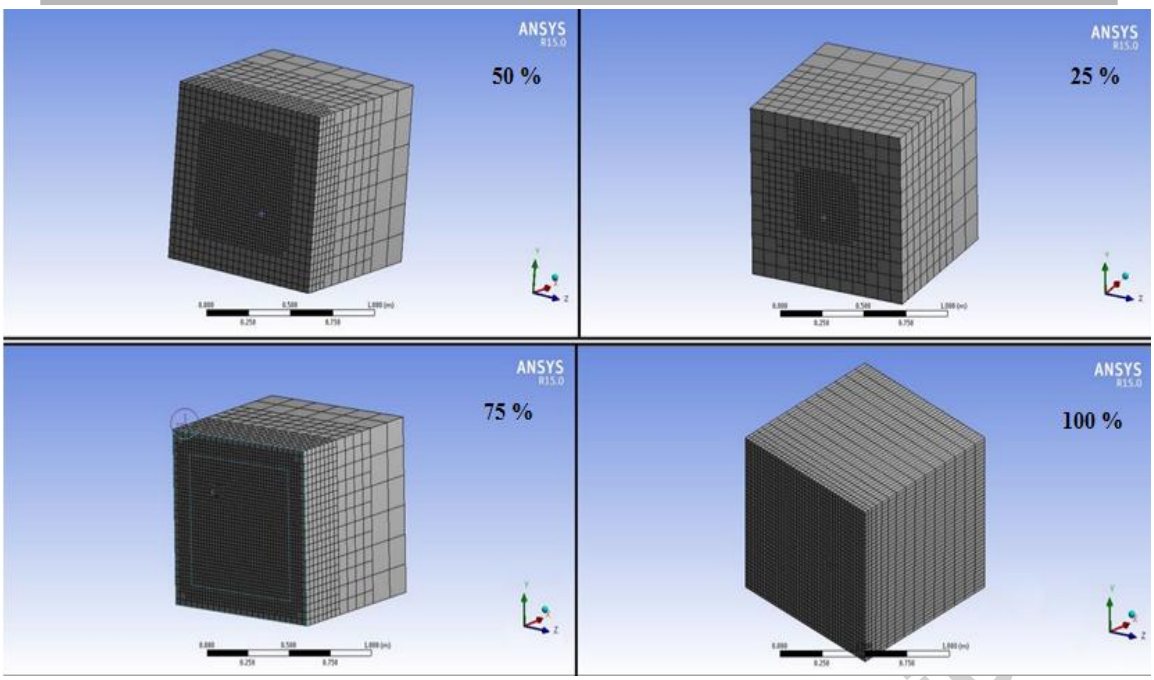

Fig. 6: Grid generation for four cases of the test rooms

Solar load model provided by FLUENT can be utilized to determine radiation actions from the solar radiation that enters an experimental room. This model contains a solar calculator technique can be utilized to determine the location of the sun in the sky at any time and position. Solar load is only obtainable in the three dimensions solver and can be utilized to model steady and unsteady problems. In the analysis of buildings, solar loading supplying a considerable encumbrance on the cooling and heating demand in the four-season conditions. The second order scheme was used for solving the momentum and energy equations.

The body-force-weighted discretization is recommended for solving the high Rayleigh number flows. Therefore, body force weighted was used to discretize the pressure term. Pressure-velocity coupling was achieved using the Pressure-Implicit with Splitting of Operator algorithm (PISO). PISO is recommended for transient flow calculation [17]. Under-relaxation factors were applied in order to control the changes of variable values between successive iterations and avoiding divergence of the solutions. During the resolution of equations, the typical values of the under-relaxation parameters used were approximately 0.3 for pressure, 0.7 for momentum, and 0.8 for energy and density. The (k-ε) turbulence model was an important model used in this study to simulate the natural convection for turbulent flow inside the test rooms [24]. It was a two-equation model which gave a general flow description. The convergence criteria for the solution (velocities, pressure, concentration) and energy are 10^{-3}, 10^{-6} respectively. In Fluent the time-dependent equations must be discretized in both space and time. Temporal discretization involves the integration of every term in the differential equations over a time step Δt .

The integration of the transient terms is straightforward, as shown below:

$$\frac{\phi^{n+1}-\phi^{n}}{\Delta t}=f(\phi) \quad (7)$$

For natural convection problems, Boussinesq model was used to get faster convergence. This model considers density as a stable value in all solved equations, except for the buoyancy expression in equation 3. The following hypotheses were assumed to solve the problem[24]:

1- The natural convection in the room is turbulent and dependent on time.

2- All water properties are constant except density based on Boussinesq model as:

$$\rho \cong \rho_o * (1+\beta * (T_o - T)) \quad (8)$$

3- Choose the (PISO) algorithm to link the momentum and energy equations suitable for time-dependent situations.

4- Choose the Body Force Weighted Scheme to solve the pressure term in the momentum equation.

5- Initial and boundary conditions were determined as:

- Initial condition: For time t = 0, temperature of water = 20 ^{o}C.
- Boundary condition: The solar beam irradiation at the experimental rooms was calculated using fluent solar calculator model depending on the time, date, and position. All faces were affronted except the south face and in some tests; the west face was subjected to solar irradiation. The flow boundary conditions that are needed for all sides. A non-slip condition is ascribed to fluid velocity at all the internal solid walls and the shear stress is calculated considering smooth surfaces.

Rayleigh number less than 10^8 indicate a buoyancy-induced laminar flow, with transition to turbulence occurring over the range of (10^8< Ra < 10^{10}). When it is required to solve a high-Rayleigh-number flow (Ra >10^8), an iterative procedure should be followed to get best results. The main steps are given below:

1. Start the solution from a steady-state solution obtained for the same or a lower Rayleigh number.

2. Determine the time constant as[25]:

$$\tau = \frac{1}{\sqrt{g * \beta * \Delta T * L}} \quad (9)$$

Where: L is the length scale (height of test room). Use a time step Δt such that:

$$\Delta t \cong \frac{\tau}{4} \quad (10)$$

Utilizing a larger value of Δt may lead to divergence.

4. Results and Discussions:

This section discusses the experimental and numerical results of the tests; temperature distribution and velocity magnitude within the test rooms. In addition, this study made a comparison between the experimental results and result of the (ANSYS - FLUENT) numerical analysis.

4.1 Parametric Mean Temperatures:

The thermal performance of the test rooms was analyzed as the glass window was directed southward to investigate the effect of a window orientation. The inside room temperature is an important parameter. It is defined as a mass weighted average temperature, which is calculated by the equation given as:

$$T_{av} = \frac{\sum_{i=1}^{n} M_i * T_i}{M_{total}} \qquad (11)$$

The variation of inside room temperature through summer solstice day (21-June) is shown in Fig. 7. It was noticed that the mean air temperature inside the test room increased with time up to 2 p.m. and then decreased. This is because the heat losses become just larger than the solar radiation. This agreed with experimental results of most studies [6]. The mean value of the air temperature of the different test rooms was different depending on the time and window size as can be noticed experimentally from Table 2. The ultimate value of room temperature depends on the solar radiation, the predominant weather conditions and heat losses [9]. The room that has conventional 25% south window size is a favorite in the hot climate (Iraq) [2]. The correspondence between the simulation data and the experimental results is acceptable as is evident in Fig. 8. The difference between the Fluent and the experimental results is less than 5% for the insides air a temperature, which is considered an acceptable result. The maximum value of the room temperature and time of its evolution were diverse for the different days as can be noticed practically from Fig.9.

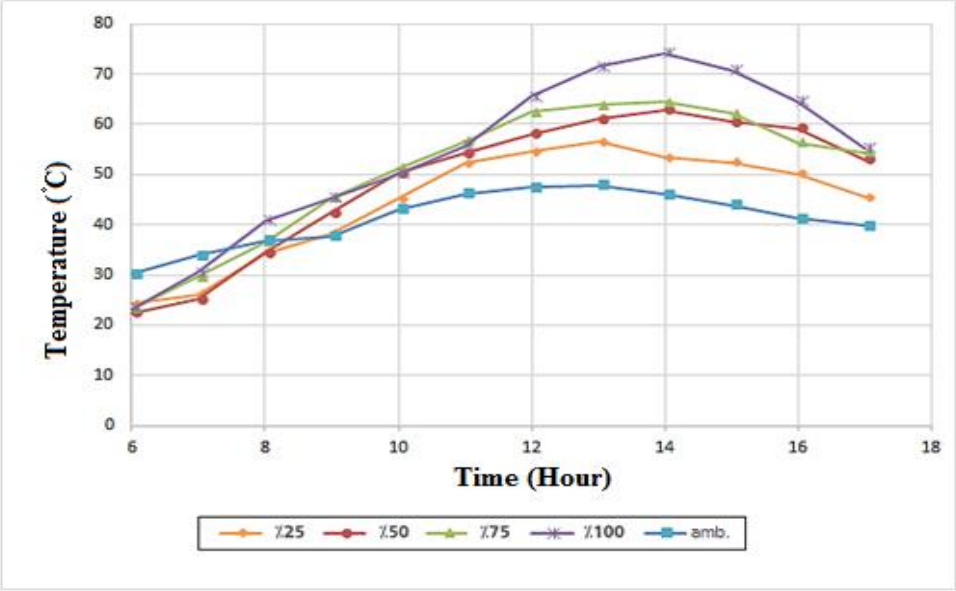

Fig. 7: Variation of the inside air temperature for different window sizes at south orientation

The ultimate value depended on the solar radiation value, the weather conditions, the inside air temperature at the beginning and the heat losses, which are different during the spring and summer

months [14]. The ultimate value was 58 ^{o}C on the summer solstice day and reached 54 ^{o}C for spring equinox day. The temperature changes of the test rooms when the windows face the west are shown in Fig.10. The temperature variation in this status is identical to the previous case.

Table 2: Effect of the window size on the mean air temperature

Window size (%)	**Room air temperature (^{o}C)**					
Time	8 A.M		1 P.M.		5 P.M.	
Direction	South	West	South	West	South	West
25%	35	34	57	55	45	42
50%	35	35	61	63	53	45
75%	37	41	64	67	54	47
100%	41	42	72	75	55	49
Ambient temperature (^{o}C)	37	37	48	46	40	39

4.2 Temperature distribution:

Figures 11 to 12 have a significant attention. They show the temperature distribution of air in the experimental rooms at different times through the operation day. Fig. 11 shows the three-dimensional temperature distribution in the experimental room with window area equals 25% at different times. There were large thermal gradients inside the room. The air was stratified; the figures also show the variation of the air temperature distribution in the room during the day. During the first hour, the lower part of the room was nearly at a lower temperature while the temperature difference across the room was small. During the mid-part of the operation period, the difference increases between the temperature of the top and bottom of the experimental room. The large thermal gradient was confined to window equal to 25% of the wall due to its small area as illustrated in Figures. 11a,b, and c, while in the rooms with 75% window, the thermal gradient in the room was better and the distribution of heat was regular inside the room. Increasing the window size caused an increase in the heat transfer rates throughout the body of the air and variation in the air density. Therefore, the hot air was accumulated at the upper part of the room. The buoyancy effect caused natural circulation of the fluid particle relative to the collector solid walls. Increasing the size of the window caused a greater difference in the air temperature inside the rooms, also increasing the clarity of the thermal gradient as shown in Fig. 12. When the window is directed to the west, the temperature gradient was similar to that of the south but varied with lower temperatures because less solar radiation entered before midday, leading to lower air temperatures. In the afternoon, the inside air temperature to the west direction was higher than the south direction because more solar radiation entered the window.

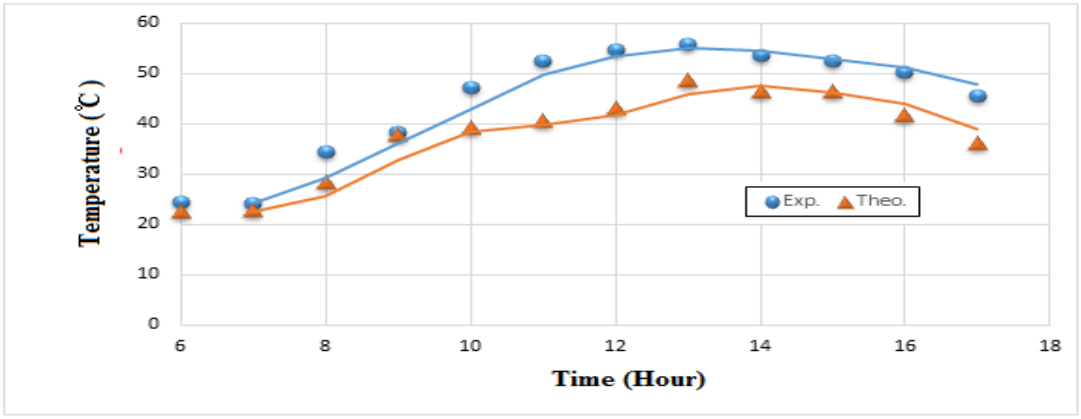

(a) Window size (25%)

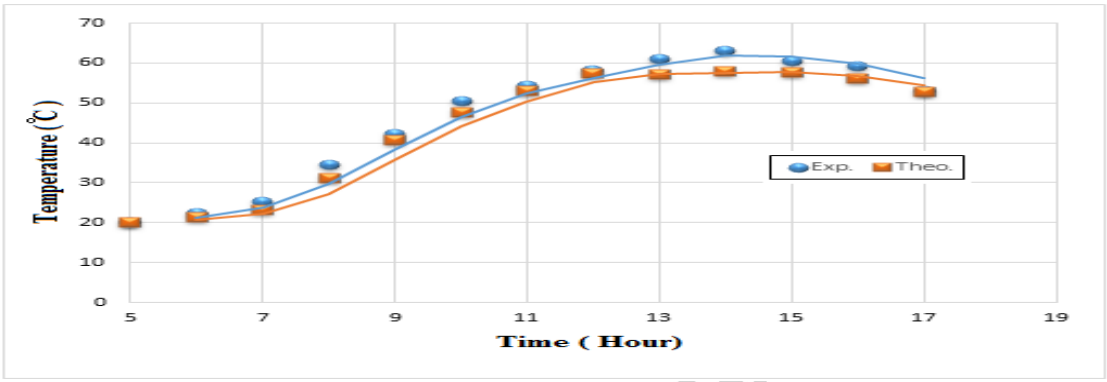

(b) Window size (50%)

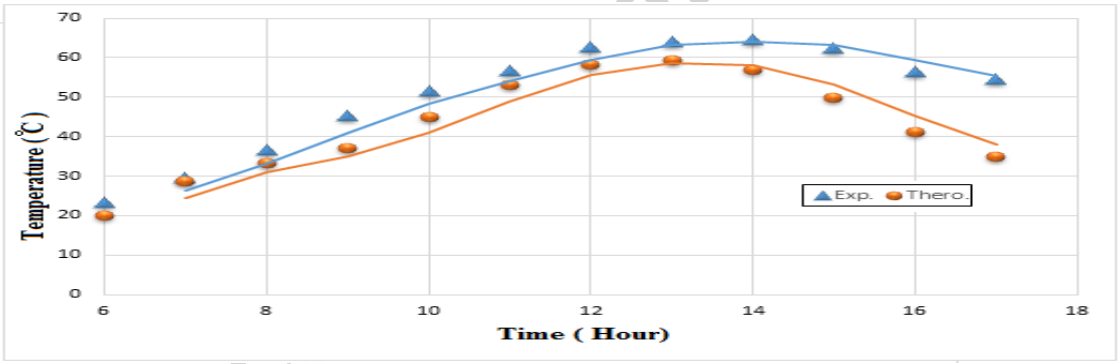

(c) Window size (75%)

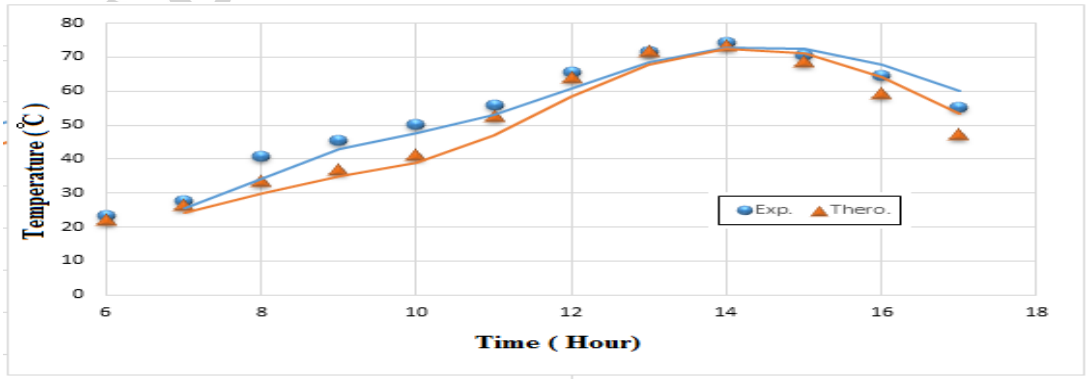

(d) Window size (100)

Fig. 8: Comparison of experimental and numerical room temperature for south orientation.

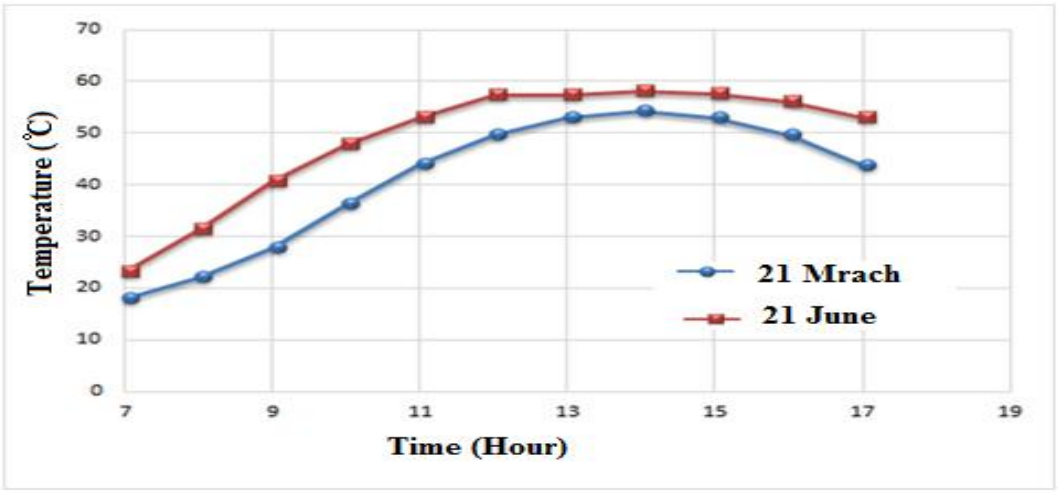

Fig. 9: The variation of room temperature through the spring and summer seasons.

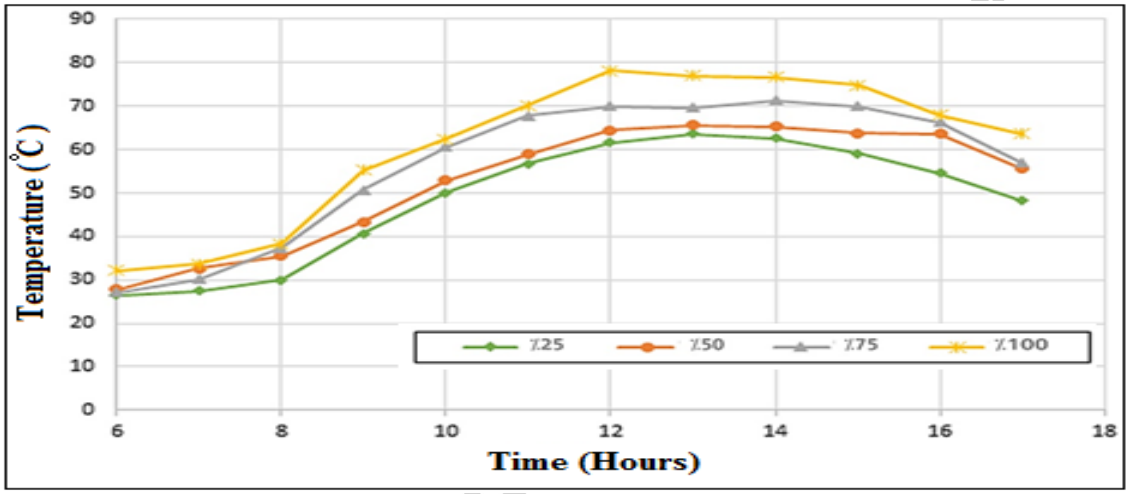

Fig. 10: Effect of window size on the inside air temperature for west orientation

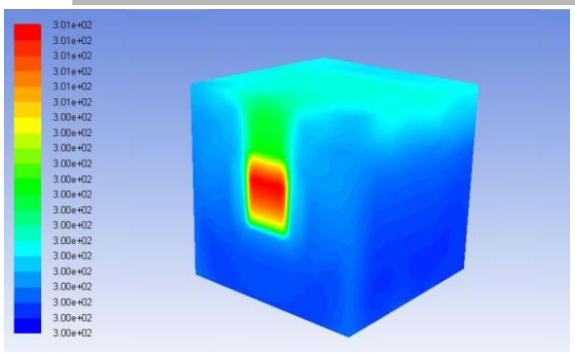

Window size 25%

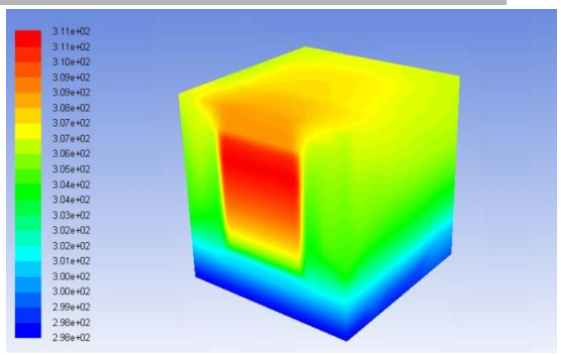

Window size 75%

(a) **At 8 A.M.**

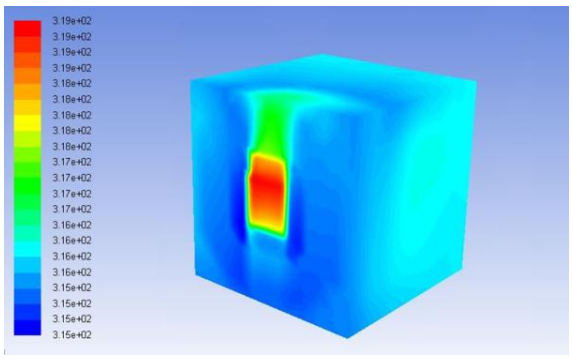

Window size 25%

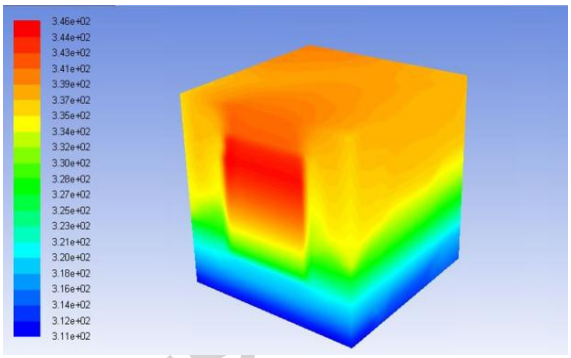

Window size 75%

(b) **12 noon**

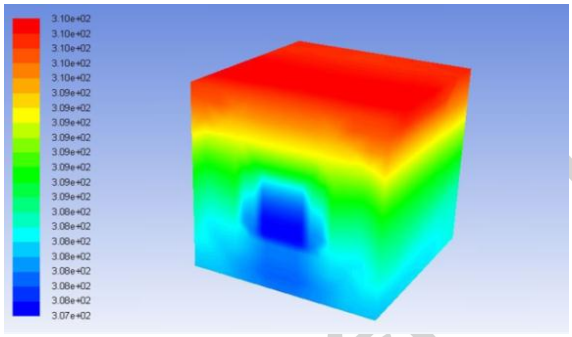

Window size 25%

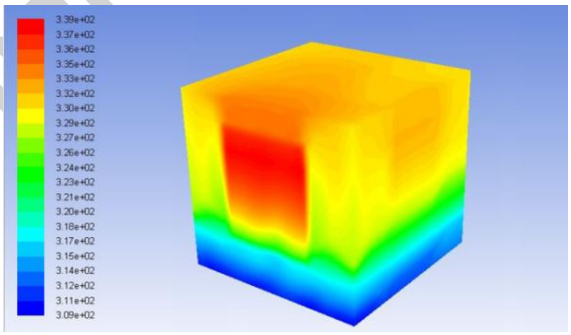

Window size 75%

(c) 5 P.M.

Fig. 11: Temperature distribution for the 25% and 50% windows sizes at different times

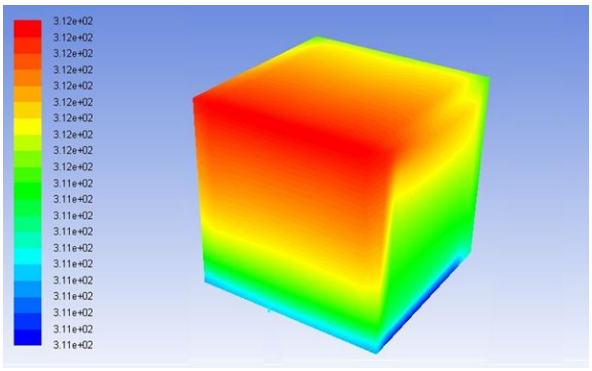

Fig. 12: Temperature distribution for the 100% windows size at 5 p.m.

4.3 Convection Flow Patterns:

Incident solar radiation motivated heat transfer throughout the body of the water with a performing change in the air density. The buoyancy effect caused natural flow of the air relative to the test room solid walls. The operation was uninterrupted as long as there was a heat flux. A three-dimensional simulation of the track of the particles colored by its speed was given, especially the air particle movement inside the rooms at 12 noon when the window directed 25% to the south and west to obtain more information about the motion of the air inside the test room as shown in Fig.13. The fluid rose under the effect of buoyancy forces. Some particles turned towards the interior of the collector because do not have enough kinetic energy to continue upwards. The particles in contact with the glass surface rose under the effect of buoyancy forces, while the other particles reached the top of the collector and then turned down. These particles followed the a-b-c-d path (Fig. 13a). The figure shows a laminar air flow in the test room as a result of the low value of Rayleigh number in this region. The fluid movement was similar when the window was oriented towards south and west. With the increasing air temperature, the influence of turbulence began to appear as shown in Fig. 14b. The magnitude of the velocity was also increased by increasing the window size and solar radiation as shown in Figures 14a, b, c, and d. Table 3 shows the magnitude of the mean velocity inside the experimental rooms at 12 p.m. It was noted that the airspeed increased with the increasing window size, which led to the entry of a large amount of solar radiation entering the room that causes heating the air molecules inside the rooms. The movement of air inside the room was low due to the lack of solar radiation coming through the room window which heats heating air molecules.

Table 3: Mean velocity of air inside room when the window faced to south

Window size (%)	Mean air velocity (m/s)
25%	0.157
50%	0.329
75%	0.359
100%	0.384

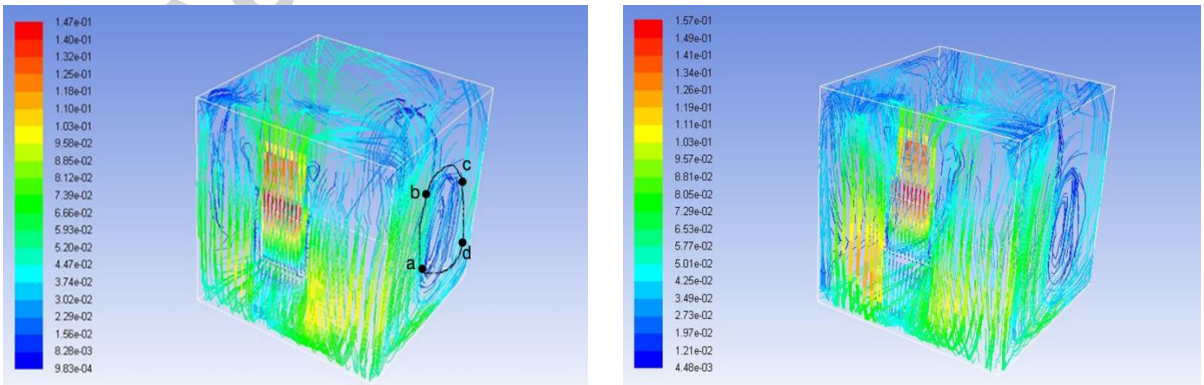

(a) South orientation **(b) West orientation**

Fig. 13: Air particle movement at 12 noon and 25% of window size.

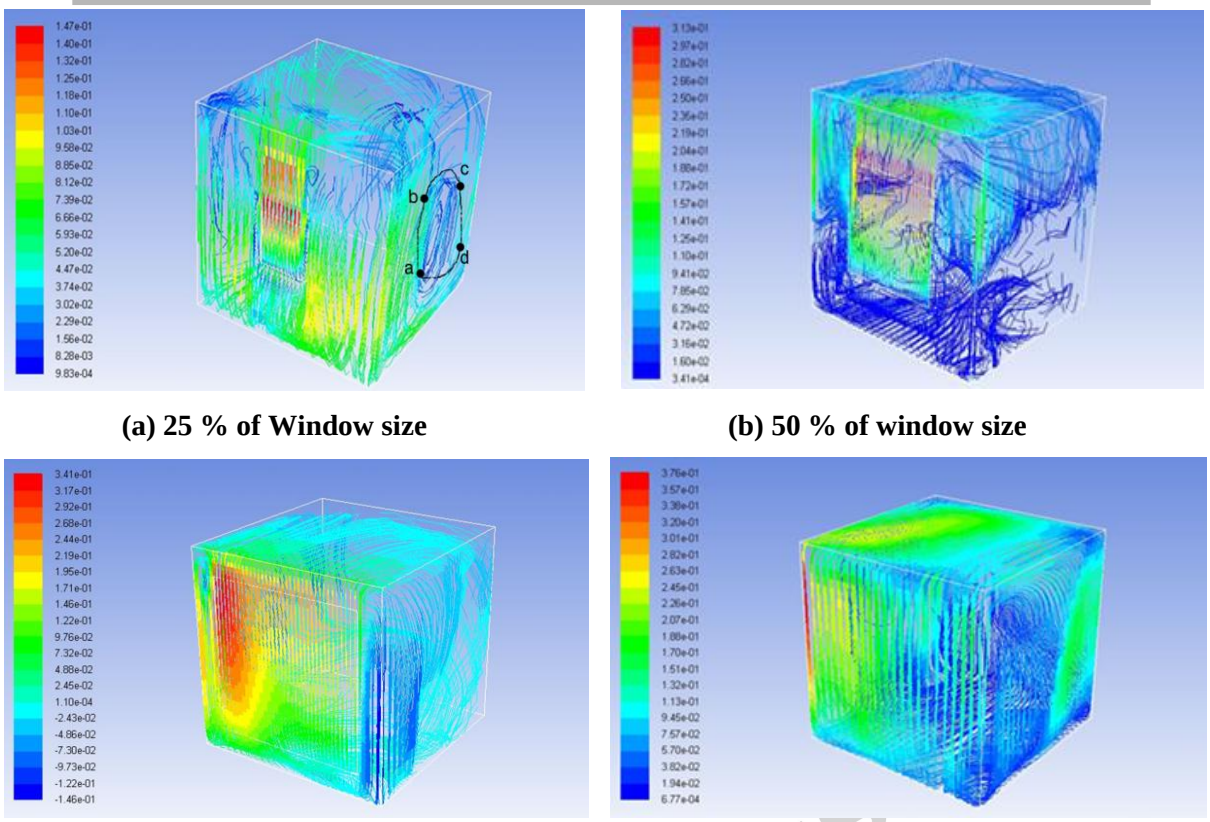

(a) 25 % of Window size **(b) 50 % of window size**

(c) 75 % of Window size **(d) 100 % of window size**

Fig. 14: Velocity path line for different window size at 12 p.m.

5. Conclusions and Recommendation:

The purpose of this paper is to determine the effect of window size and its orientation on temperature distribution and air movement in Iraq to minimize cooling load in rooms from the point of view of climate influences. According to the results presented in the previous sections, the following conclusions can be obtained:

1- The room that has conventional 25% south window size is a favorite in the hot climate (Iraq).

2- The results show the positive effect of directing the window to the south compared to the west. It was noticed that the average of air temperature inside test room increased with time until 2 p.m. and then decreased.

3- The thermal performance of the rooms during the night was approximately equal in all direction of the window.

4- Increasing the window size caused an increase in the heat transfer rates throughout the body of the air and variation in the air density.

5- When the window directed to the west, it is recommended to reduce the window size as much as possible, where the less window area leads to a high thermal performance of the room and reduce the consumption of electricity. All the effects give an economic benefits to the endures and energy consumption.

6- The fluid movement was similar when the window was oriented towards the south and the west. With increasing air temperature, the influence of turbulence began to appear. The magnitude of the velocity was also increased by increasing the window size and solar radiation.

6. References:

[1] O. K. Ahmed and A. H. Ahmed, *Principles of Renewable energies*, First edit. Baghdad: Foundation of technical education, 2011.

[2] M. N. Inanici and F. N. Demirbilek, "Thermal performance optimization of building aspect ratio and south window size in five cities having different climatic characteristics of Turkey," *Build Environ*, vol. 35, no. 1, pp. 41–52, 2000.

[3] S. Nikoofard, V. I. Ugursal, and I. Beausoleil-Morrison, "Effect of window modifications on household energy requirement for heating and cooling in Canada," in *The Canadian Conference on Building Simulation*, 2012, no. 2006, pp. 325–337.

[4] L. Ma, N. Shao, J. Zhang, and T. Zhao, "The Influence of Doors and Windows on the Indoor Temperature in Rural House," *Procedia Eng*, vol. 121, pp. 621–627, 2015.

[5] M. Vedavyasa, M. S. Rajagopal, and L. K. Sreepathi, "Experimental Study on Effect of Window Location and Surface Absorptivity on Temperature inside an Enclosure," *Int Res J Environ Sci*, vol. 1, no. 3, pp. 27–31, 2012.

[6] S. Amos-Abanyie, F. O. Akuffo, and V. Kutin-Sanwu, "Effects of thermal mass, window size, and night-time ventilation on peak indoor air temperature in the warm-humid climate of ghana," *Sci World J*, vol. 2013, 2013.

[7] M. L. Persson, A. Roos, and M. Wall, "Influence of window size on the energy balance of low energy houses," *Energy Build*, vol. 38, no. 3, pp. 181–188, 2006.

[8] R. M. J. Bokel, "The effect of window position and window size on the energy demand for heating, cooling and electric lighting," *Build Simul*, pp. 117–121, 2007.

[9] Farraj F. Al-ajmi V.I. Hanby, "Simulation of energy consumption for Kuwaiti domestic buildings," *Energy Build*, vol. 40, no. 6, pp. 1101–1109, 2008.

[10] G. Hong, D. Kim, and B. Kim, "Experimental Investigation of Thermal Behaviors in Window Systems by Monitoring of Surface Condensation Using Full-Scale Measurements and Simulation Tools," *Energies*, vol. 9, no. 11, p. 979, 2016.

[11] S. bin A. A. Al-Sudais, "The Effect of Glass Windows, Orientation, Area and Types on the Thermal Performance of the Internal Spaces of the Buildings in Hot-Dry Regions,An Experimental Case Study: Test Cells at The educational Farm – KSU - Riyadh," King Suad university, 2010.

[12] N. F. Antwan, "Effect of Window Over-Hang in Iraqi Building on Cooling Load," *Eng Technol*, vol. 25, no. 7, pp. 940–949, 2007.

[13] K. C, E. C, and N. J, "Passive Analysis of the Effect of Window Size and Position on Indoor

Comfort for Residential Rooms in Kumasi, Ghana," *Int Adv Res J Sci Eng Technol*, vol. 2, no. 10, pp. 114–115, 2015.

[14] S. Shaik, K. Gorantla, and A. B. T. P. Setty, "Effect of Window Overhang Shade on Heat Gain of Various Single Glazing Window Glasses for Passive Cooling," *Procedia Technol*, vol. 23, pp. 439–446, 2016.

[15] Https://weatherspark.com, "Average-Weather-in-Kirkuk," 2017. .

[16] O. K. Ahmed, "Assessment of Wind Speed for Electricity Generation in Makhool Mountain in Iraq," *Int J Inven Eng Sci*, vol. 2, no. 2, pp. 5–10, 2014.

[17] O. K. Ahmed and Z. A. Mohammed, "Dust effect on the performance of the hybrid PV/Thermal collector," *Therm Sci Eng Prog*, vol. 3, pp. 114–122, Feb. 2017.

[18] Iraqi Metrological Organization and Seismology, "Monthly average (temperature, rains, solar radiation, humidity, wind speed)," Kirkuk city, 2014.

[19] O. Khalil Ahmed and Z. Aziz Mohammed, "Influence of porous media on the performance of hybrid PV/Thermal collector," *Renew Energy*, vol. 112, pp. 378–387, 2017.

[20] Ministry of Planning, "Technical Specifications for Civil Work," Baghdad, 2014.

[21] J. P. Holman, *Experimental methods for engineers*, vol. 9, no. 2. 1994.

[22] O. K. Ahmed, A. H. Ahmed, and O. M. Ali, "Effect of the Shape Surface of Absorber Plate on Performance of Built-in-Storage Solar Water Heater," *J Energy Nat Resour*, vol. 3, no. 5, pp. 58–65, 2014.

[23] H. K. V. and W. Malalasekera, *Introduction to Computational Fluid Dynamics*, 2nd ed. Harlow, 2007.

[24] O. Khalil Ahmed, "Experimental and numerical investigation of cylindrical storage collector (case study)," *Case Stud Therm Eng*, vol. 10, pp. 362–369, 2017.

[25] I. ANSYS, *ANSYS Fluent Tutorial Guide*, vol. Releas 15., no. 1. Canonsburg, 2013.

Highlights

- The purpose of this paper is to determine the size of the window on the temperature distribution and air velocity of rooms.
- The experimental investigation contained manufacturing four test rooms where the window areas were 25%, 50%, 75%, and 100% from facade area.
- A numerical analysis was carried out using the Fluent software. The Fluent results agreed well with the experimental data obtained.
- The room with 25% of the facade had the best performance in comparison with other designs.